CONTINUOUS MONITORING OF SPECTRAL FEATURES
OF ELECTRON BEAM ORBIT MOTION AT NSLS-II*

B. Podobedov[†], A.A. Derbenev, K. Ha, T.V. Shaftan,
Brookhaven National Laboratory, Upton, NY 11973

Abstract

NSLS-II ring is equipped with state-of the art beam position monitors (BPMs) which are indispensable in all aspects of machine studies and operations. Among other data, they can provide, on demand, up to 10 seconds of fast-acquisition (FA) data, sampled at ~10 kHz. Analysis of these data in time, frequency and spatial domains provides valuable insights into orbit stability, locations of residual noise sources, performance of feedback systems, etc. In addition, changes in FA signal spectral features are often the earliest indicators of potential equipment problems. This is why we recently implemented an Input / Output Controller (IOC) software that runs during regular user operation, and, once a minute, acquires 10 second buffers of FA data from 180 BPMs around the ring. These buffers are processed to determine the amplitudes and frequencies of the strongest spectral peaks as well as some other measures of fast beam orbit noise. Processed results can be monitored in real time and are also archived for offline analysis and troubleshooting. In this paper we discuss the implementation of this system and the insights we gained from it over about two years of operations.

INTRODUCTION

NSLS-II is the latest third-generation light source in the United States, located at Brookhaven National Laboratory [1,2]. Since the storage ring commissioning in 2014, the stored beam current for routine user operation was gradually raised to 400 mA, with top off injection. Because beam stability is of paramount importance for the users, from the very beginning of NSLS-II meticulous attention was paid to all aspects of machine design and operation that have potential impact on beam stability. State-of-the-art RF BPM receivers were designed and built in-house [3,4] to provide the capability to monitor beam orbit with unprecedented resolution. Among other data streams, BPMs provide 10-kHz sampled orbit FA data to another state-of-the art system, Fast Orbit Feedback (FOFB) [5], which currently suppresses orbit noise up to 200 Hz to the level below 10% of the beam size in the vertical and ~1 % in the horizontal plane. Together with other active stabilization systems, such as RF-frequency feedback [2] and local bump agent [6], FOFB also maintains long-term drifts at the ID source points at the few micron / few microradian peak-to-peak over a 24-hour period.

While monitoring long-term orbit drifts is conceptually simple (10-Hz data from all BPMs are routinely archived), the case of fast orbit motions is not straightforward. First

of all, FA data rates all but prohibit efficient archiving. Second, the sheer volume of data calls for some automated data processing, which extracts some key stability metrics that are suitable for human analysis. For fast orbit motions, these metrics are most conveniently constructed in the frequency domain, i.e. noise line peak amplitudes and frequencies. Reducing FA data from hundreds of BPMs to a handful of metrics inevitably requires data decimation or averaging in space, frequency or time domains. In this paper we present the solution we arrived at and implemented in the so-called "Orbit Monitor IOC".
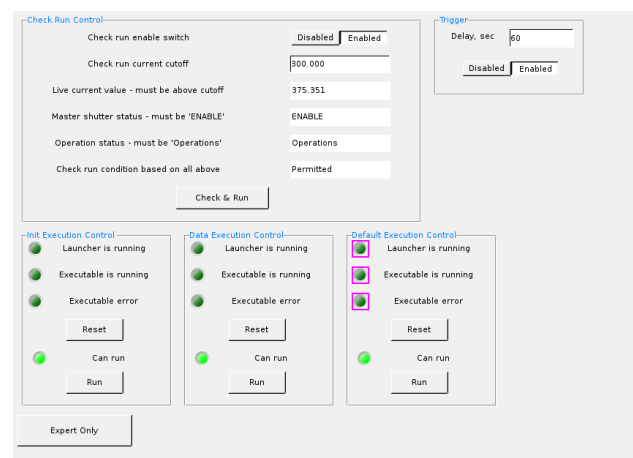
IOC IMPLEMENTATION

Figure 1: Orbit Monitor IOC control menu.

The IOC runs continuously, unless it is disabled (which is uncommon) from the lead Operator console using the control menu shown in Fig.1. However, since the IOC is mainly geared for characterization of fast orbit stability during user operations, it only saves the data when the ring is in operations, shutters are enabled, and the beam current is above certain threshold (typically set at 300 mA). Under these conditions, every minute, all 180 "regular" BPMs are triggered, and a 10-second buffer of synchronized FA data is acquired. The buffer is subsequently converted to the frequency domain, and the resulting spectra are averaged over three groups of BPMs, horizontal dispersive (a total of 60), horizontal non-dispersive (120), and vertical (179). An example of these averaged spectra (PSD) for the horizontal plane is presented in Fig. 2.

Each of the three resulting spectra is then processed by the IOC to find the amplitudes and frequencies of the 10 highest spectral peaks (separated by at least 10 Hz from each other and from zero). The resulting amplitudes and frequencies are written into corresponding EPICS Process Variables (PVs), which could be monitored (alongside any

other machine PVs) in real time in the Control System Studio (CSS) data browser. Separately, 10-second average rms noise values for each of the three groups of BPMs (these are essentially equivalent to [0.1-5000] Hz integrated PSD in the frequency domain) are also calculated and written into PVs. Finally, all PVs updated by the IOC are archived once a minute.
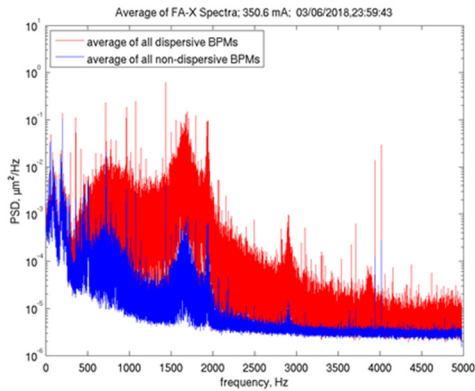

Figure 2: Example of average BPM spectra in the horizontal plane. Frequency-integrated PSD values are 2.6 μm (dispersive BPMs) and 0.6 μm for non-dispersive. These are on the order of 1% of the horizontal beam-size.

On top of archiving the processed values, derived from the orbit noise spectra as described above, every 24-hour period of operations the system saves a "raw data" file, i.e. 10 seconds of synchronized FA data for 180 BPMs. These files contain all the information to give a comprehensive snapshot of fast orbit stability around the machine. They provide the ability to localize AC orbit perturbations around the ring; they allow for detailed spectral or time-domain analysis of orbit noise, and in general, they also help to paint a more complete picture as to how the orbit noise evolves over the long term.

Finally, the system is configured to save additional raw data files on-demand, or if any stability-related PVs exceed pre-defined thresholds. Since the beginning we have been typically running with thresholds on average rms noise values set at 2 microns (horizontal non-dispersive and vertical) and 8 microns for the horizontal dispersive. The reasoning behind these threshold values was that they were roughly a factor of two larger than the corresponding typical rms values with stable beam. With these thresholds, the IOC was saving on average about one file per week, which shows that fast orbit perturbations that exceed twice the typical RMS are not common. Furthermore, more than a half of these files were saved a minute or so after a ring refill, when the operator would set "Beam Available" PV to ON (thus enabling the IOC to save the data) while still performing substantial local bump corrections, often with FOFB off.

IOC USE EXAMPLES

The first simple example showing the usefulness of the data provided by this IOC is illustrated in Fig 3. It shows

the results of power supply "mains compensation", performed by the RF Group to reduce the amplitudes of power line harmonics (in this case mainly 720 and 360 Hz) at the output of the RF power transmitter for cavity D. The plot shows that, for horizontal dispersive BPMs, the frequency of the highest spectral peak (brown circles) remained at 720 Hz. However, as a result of compensation, the amplitude of the 720 Hz line (blue) was reduced by one order of magnitude. This also resulted in substantial reduction of integrated rms noise, from ~3.5 microns down to ~2.8 microns (red). While this procedure is performed routinely, the RF Group used to only look at the cavity probe signals (to quantify power line amplitudes in dBc with respect to the 500 MHz fundamental RF frequency). The data provided by this IOC allows us to immediately quantify the effects of the compensation procedure on beam orbit noise, as well as to recommend if and when such compensation should be performed.
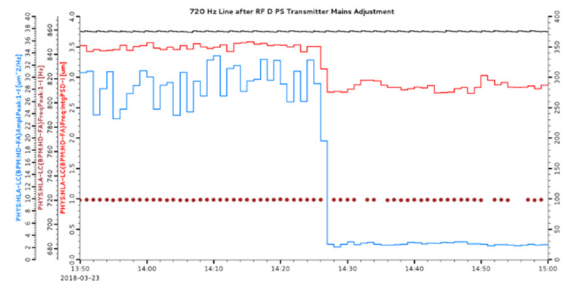

Figure 3: The amplitude of the highest spectral peak (blue), the frequency of that peak (720 Hz, brown circles), and the rms noise amplitude (red) for horizontal dispersive BPMs during cavity D RF transmitter power supply "mains compensation". 375 mA top-off current is shown in black.

Our next example demonstrates the IOC capabilities in providing global fast orbit stability characterization over reasonably long timescales, i.e. weekly, such as shown in Fig. 4. The archive plot, showing a typical stability behavior, illustrates that the orbit noise at horizontal non-dispersive BPMs and at vertical BPMs remained at a fairly constant level, while the dispersive BPMs (red) showed more variation. The reasons behind significant spikes (in addition to the ones right after the beam dumps) are marked in the plot. We found this ability to plot, analyze and correlate fast orbit noise-related quantities such as the ones shown, to be very helpful.
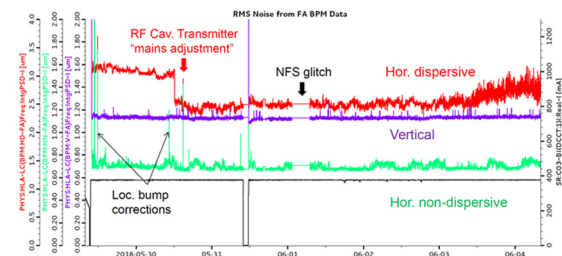

Figure 4: A one-week history of [0.1-5000] Hz integrated PSD for hor. dispersive (red), hor. non-dispersive (green) and vertical (purple) BPMs. "NFS glitch" marks a network failure preventing the IOC from saving data.

In the next example we show how the IOC helps to diagnose fast orbit transients when these exceed pre-defined thresholds as described earlier. A time-domain plot of one of these auto-generated files (only vertical BPMs are plotted) is shown in Fig. 5 (left). This file was automatically saved by the IOC because the vertical rms exceeded 2 microns. This happened when the Insertion Device (ID) Group was fixing the Cell 2 ID "undulator taper" (a mechanical issue with the ID gap control which was successfully accomplished without interrupting user operations, but did produce a large orbit spike). 100-micron scale orbit perturbations at the time around 7 seconds are clearly visible in the figure. The orbit difference before and after the adjustment is plotted in Fig. 5 (right), showing, as expected, a vertical orbit spike around Cell 2.
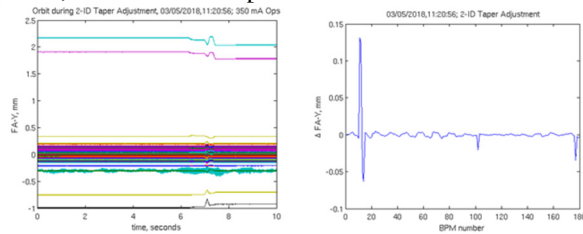

Figure 5: (left) Vertical positions from the FA orbit file automatically saved by the IOC during 2-ID taper adjustment; a 100-micron scale perturbation at time ~7 seconds is clearly visible. (right) Orbit difference before and after the adjustment showing the perturbation around Cell 2.

More complicated examples of threshold-triggered file saves by this IOC included jumps in the master oscillator frequency (the issue subsequently addressed by the RF Group), various instances of imperfect orbit corrections, FOFB turn-offs, and BPM failures. In that regard, the IOC proved not only useful to monitor and diagnose potential issues with fast orbit stability, but also as a diagnostics tool for various hardware systems, for which relatively subtle failures may first show up as fast beam orbit perturbations.

For our final example we describe a more complicated orbit noise issue, which the IOC helped to diagnose, but without fully revealing the mechanism behind it.

At the beginning of the user run in January of 2018, the IOC-produced data (similar to that shown in Fig. 1) revealed a new and rather distinct spectral feature in fast beam orbit noise. Specifically, it was a ~200 Hz narrow line, frequently, but not always, observed in horizontal non-dispersive BPMs. When present, the line was either the highest or the second highest (after 60 Hz) peak in the PSD, although its contribution to the total integrated rms noise of this group of BPMs was very minor. Also, while clearly visible on BPMs, the amplitude of the corresponding orbit perturbation was too small to be noticed by the users. Applying SVD-based response matrix inversion (see e.g. [7]) to one of the 10-sec raw data file saved by the IOC, we were able to localize the source of this orbit perturbation to Cell 19 ID straight. After that, scanning the 19-ID (NYX) undulator gap, we noticed that the 200 Hz line would only appear when the ID gap was close to the minimum value of 6.4 mm, as illustrated in Fig. 6.

Figure 6: The frequency (red circles) and amplitude of the highest (brown) and the 2nd highest (green) spectral peaks for hor. non-dispersive BPMs. The 19-ID (NYX) undulator gap (blue) is fully opened and then fully closed.

This figure shows that, for horizontal non-dispersive BPMs, the frequency of the highest spectral peak changed from 200 Hz, when the ID gap was fully closed, to 60 Hz, when the ID gap was open to 20.3 mm. Meanwhile, with the gap opening, the amplitude of the highest spectral peak went down, to the level of (originally) the 2nd highest spectral peak, which was the 60 Hz line, unaffected by the undulator gap. We emphasize that while a similar analysis could have been performed "by hand", starting from FA BPM data obtained by other means, plotting the archived PVs provided by the IOC (together with all other relevant PVs) has made the analysis a lot more efficient).

The gap dependence explained the intermittent nature of the noise source (users were occasionally opening the gap), but not its mechanism. A separate investigation traced the most likely cause of the perturbation to a powerful external mechanical pump, model number ACP-15 Adixen/Pfeiffer, which had to be temporarily installed on the floor right next to the undulator. The pump, connected to the undulator chamber by a metalized corrugated vacuum hose, was needed to counteract an insulating vacuum leak from the internal cooling water lines in the undulator. The 200 Hz line disappeared right after the March 2018 maintenance period, during which the undulator (and the pump) were removed from the ring for repairs. When the refurbished, leak-less and no longer needing an external vacuum pump undulator was re-installed during the Spring 2018 shutdown, the 200 Hz line did not come back.

CONCLUSION

We recently implemented the Orbit Monitor IOC, which acquires snapshots of 10-kHz orbit data, processes them to extract key spectral features, and archives the results at one-minute intervals during NSLS-II user operations. This IOC has been running in its present configuration since January 2018. The IOC proved to be very useful for troubleshooting fast orbit stability issues, analyzing their causes, and documenting stability-related accelerator performance. Future developments will include potentially enhancing the present data processing, which is based on simple statistical techniques, with some machine learning algorithms.

REFERENCES

[1] F. J. Willeke, "Commissioning of NSLS-II", in *Proc. IPAC'15*, Richmond, VA, USA, May 2015, pp. 11-16. doi:10.18429/JACoW-IPAC2015-MOYGB3

[2] G. M. Wang, "Operation and Performance of NSLS-II", in *Proc. IPAC'18*, Vancouver, Canada, Apr.-May 2018, pp. 1312-1315. doi:10.18429/JACoW-IPAC2018-TUPMF030

[3] K. Vetter *et al.*, "NSLS-II RF Beam Position Monitor", in *Proc. PAC'11*, New York, NY, USA, Mar.-Apr. 2011, paper MOP211, pp. 495-497.

[4] K. Vetter *et al.*, "NSLS-II RF Beam Position Monitor Update", in *Proc. BIW'12*, Newport News, VA, USA, Apr. 2012, paper WECP02, pp. 238-241.

[5] Y. Tian, "NSLS-II Fast Orbit Feedback System," presented at the 1st BES Light Sources Beam Stability Workshop, Berkeley, CA, USA, Nov. 2018.

[6] Y. Hidaka *et al.*, "Improvements in Long-Term Orbit Stability at NSLS-II", in *Proc. IPAC'19*, Melbourne, Australia, May 2019, pp. 4070-4073. doi:10.18429/JACoW-IPAC2019-THPRB104

[7] S. Krinsky, "Global Orbit Correction", in *Handbook of Accelerator Physics and Engineering*, A. Chao and M. Tigner, Ed. Singapore: World Scientific, 1999. doi:10.1142/3818